The Meteorological Magazine

March 1991

Rainfall distribution around Athens

Comparison of UK road ice models

HMSO

Met.O.998 Vol. 120 No. 1424

First published 1991

HMSO publications are available from:

HMSO Publications Centre
(Mail and telephone only)
PO Box 276, London, SW8 5DT
Telephone orders 071-873 9090
General enquiries 071-873 0011
(queuing system in operation for both numbers)

HMSO Bookshops
49 High Holborn, London, WC1V 6HB 071-873 0011 (counter service only)
258 Broad Street, Birmingham, B1 2HE 021-643 3740
Southey House, 33 Wine Street, Bristol, BS1 2BQ (0272) 264306
9–21 Princess Street, Manchester, M60 8AS 061-834 7201
80 Chichester Street, Belfast, BT1 4JY (0232) 238451
71 Lothian Road, Edinburgh, EH3 9AZ 031-228 4181

HMSO's Accredited Agents
(see Yellow Pages)

and through good booksellers

3 8078 0010 2479 5

The Meteorological Magazine

March 1991
Vol. 120 No. 1424

551.577.21(495)

Spatial distribution of rainfall in the Greater Athens Area

G.T. Amanatidis, C. Housiadas and J.G. Bartzis
National Center for Scientific Research Demokritos, Institute of Nuclear Technology and Radiation Protection, 15310 Ag. Paraskevi Attikis, Greece

Summary

The annual and seasonal spatial distribution of rainfall in the Greater Athens Area in Greece is studied using the rainfall data from 24 rain-gauges for 1985–89. Both these rainfall distributions and the temporal variations of rainfall during the 5-year period present strong discrepancies among the different parts of the examined area. The influence of the complex topography and the atmospheric circulation on the rainfall distribution pattern for different seasons is examined. Finally, the relation of rainfall amounts to the station height above mean sea level is also investigated.

1. Introduction

The knowledge of the spatial distribution of rainfall is of interest not only from a meteorological viewpoint, but also for its importance in different fields such as agriculture, hydrology, water resources, atmospheric pollution or even in flood control. The estimation of the spatial distribution of rainfall is a complex task, especially in cases where detailed information concerning the impact of local topography on the dominant atmospheric circulation is not available. The problem becomes even more complicated by the varying pattern and intensity of near-surface atmospheric circulations.

In the case of the Greater Athens Area (GAA) (see Fig. 1) the knowledge of the spatial distribution of rainfall is rather limited though rainfall measurements have been carried out in the city of Athens for well over 130 years. One of the longest series of rainfall measurements in south-eastern Europe is that collected by the Meteorological Institute of the National Observatory of Athens (MINOA). This has been extensively analysed in the last 15 years (Katsoulis *et al.* 1976, Zerefos *et al.* 1977, Repapis 1986, Katsoulis and Kambezidis 1989), but since the knowledge is based on rainfall data obtained from only one rain-gauge, nothing can be said about the spatial distribution of rainfall in the GAA. Extrapolation of the results obtained at MINOA could create serious errors caused by the complex topography effects, especially during the cold period of the year when frontal rainfall is more common. During the warm period of the year, rainfall is predominantly convective and frequently has high intensity over small areas. Such local thunderstorm activity makes data extrapolation from one station even more unreliable.

In this study, the rainfall measured by 24 rain-gauges in the GAA for the 5-year period 1985–89 are analysed, in order to study the spatial distribution of rainfall in this area. The network used consists of all the reliable rain-gauges in operation for the examined period and covers the area in a mesoscale range. Although the results do not have an adequate climatological signific-

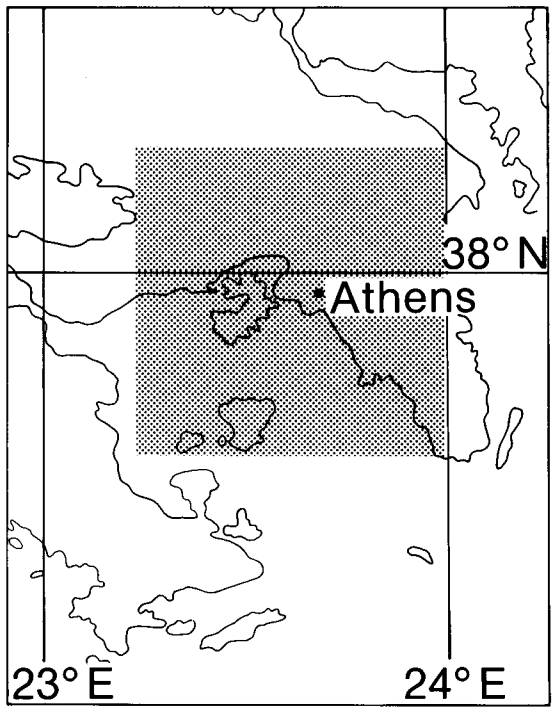

Figure 1. Map of the Attika peninsula. The Greater Athens Area is indicated by the shaded domain.

ance, because of the relatively short examined period, they confirm the expected strong irregularity of rainfall distribution in the GAA.

The results of this study may be useful in the assessment of numerical models that aim at predicting the rainfall pattern in the GAA. One such model is currently under development at the National Centre for Scientific Research (NCSR) 'Demokritos' for simulating rainfall distribution in complex topography (Housiadas *et al.* 1991). This model constitutes a further improvement of the three-dimensional atmospheric transport code, ADREA-I, developed in the context of environmental impact assessments for wind field and dispersion calculations (Bartzis *et al.* 1990, 1991).

2. Topography

The area studied in this paper is located at the south-eastern part of the Attika peninsula. The presence of mountains and sea in the GAA divide it into different regions; namely, the Athens Basin, the Thriassio Field, the Mesogia Plain, the Marathon Area and the islands of Salamina and Egina (Fig. 2).

The Athens Basin, where the city of Athens is located, is surrounded by mountains on three sides, while to the south there is sea (Saronikos Gulf). As shown in Fig. 2,

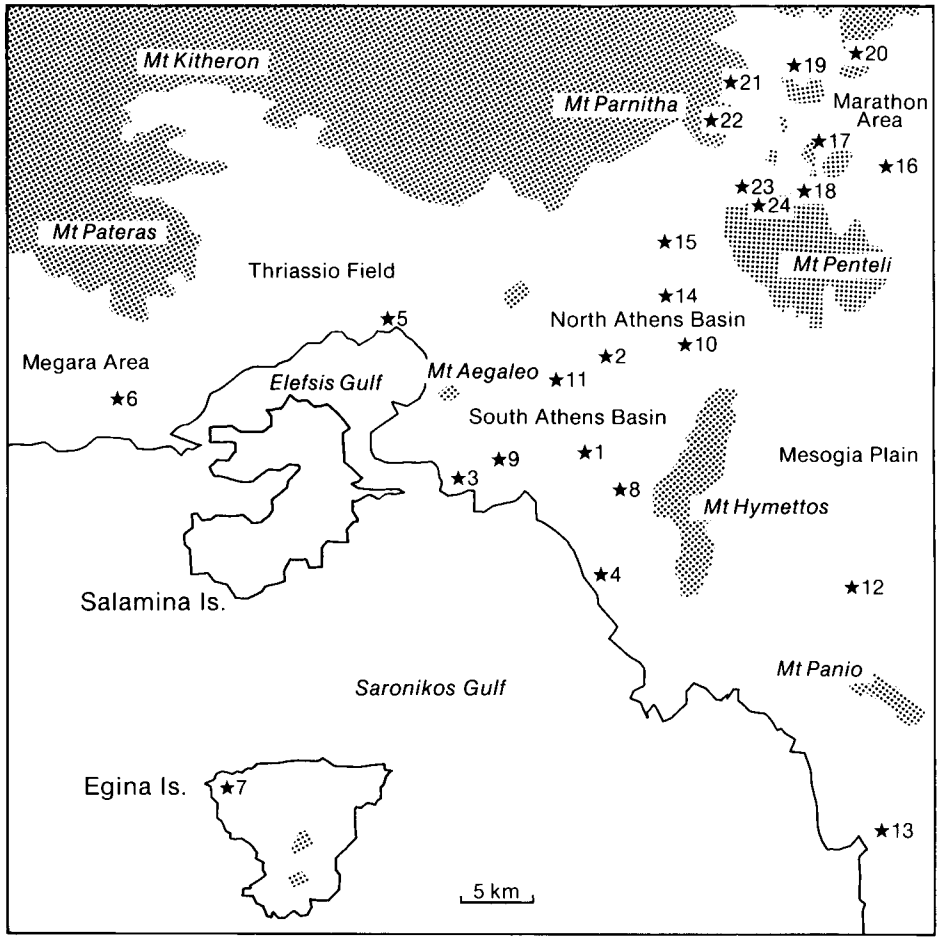

Figure 2. Map of the Greater Athens Area. Land above 400 m is indicated by shading, while the rain-gauge stations (see Table I) are indicated by numbered stars.

Mt Aegaleo (468 m) is situated to the west, Mt Parnitha (1413 m) and Penteli (1107 m) to the north and Mt Hymettos (1026 m) to the east. The Athens Basin is 30 km long and 12 km wide with a south-west to north-east major axis, and is interspersed by a series of small hills.

The Thriassio Field, located at the west side of the Athens Basin, is also surrounded by mountains. Mt Aegaleo is situated to the east, Mt Parnitha to the north, Mt Kitheron (1409 m) and Mt Pateras (1131 m) to the west, while to the south is the Elefsis Gulf coastline. Inside this area most of the Greek industry is concentrated, mainly along the coast, while inland, agricultural activities are dominant. To the east of the Thriassio Field and south of Mt Pateras extends the Megara Area, part of which is also included in the GAA.

The Mesogia Plain is located at the east of the Athens Basin and is separated from it by Mt Hymettos. Mt Penteli is situated to the north, Mt Panio (636 m) to the south, while to the east there is the Aegean Sea. Inside the plain there are some sparse industries, but agricultural activities predominate.

The Marathon Area is located to the north of Mt Penteli and east of Mt Parnitha and is washed to the north and east by the Evoikos Gulf. In the centre of the area there are the Marathon dam and the artificial homonymous lake. The lake is 250 m above mean sea level and is surrounded by forested hills.

Finally, the islands of Salamina and Egina are situated at the south-eastern part of the GAA in the Elefsis and Saronikos Gulfs respectively.

3. Climate

The climate of the GAA is Mediterranean with hot, dry summers and wet, mild winters. The summer dry period lasts for about 6 months. It begins at the end of April and continues until the beginning of October. The average daily winter temperature is 9.9 °C and the summer one is 25.8 °C. The total solar radiation is rather strong with average daily values of about 22 MJ m^{-2} in the summer and 8 MJ m^{-2} in the winter.

Most of the annual rainfall occurs in the months from October to March. This is due to the synoptic circulation which is related to extensive disturbances within the zonal westerlies (Repapis 1986). More precisely, during the summer the Atlantic anticyclone with its more northerly position dominates the Mediterranean region and therefore deflects the tracks of the storm systems. Consequently, summer is an inactive season and only infrequent local thunderstorms occur, especially in the afternoon. During the cold period of the year, this high moves to more south-westerly positions allowing depressions to enter the Mediterranean or to develop within the region. These rain-bearing depressions move from west to east (Conrad 1943, Meteorological Office 1962) and are responsible for great rainfall amounts over Greece. Contributions to the rainfall over Greece are also provided by the extension of the Siberian anticyclone over the Balkans. This creates a cold northerly airstream which, combined with possible warm and wet air masses over the central Mediterranean, produces considerable amounts of rainfall.

The upper-air flow over Greece is characterized by prevailing wind directions from the west/south-westerly sector during winter and spring, and of the northerly sector during summer and autumn (Pissimanis *et al.* 1989). Over the Athens Basin the winds tend to blow along the axis of the basin (Andreakos *et al.* 1984). The most frequent wind is that blowing from the northerly sector. The second most frequent wind blows from the south sector, while those from the east and the west sectors have a very low frequency. Except for the synoptically driven north or south winds, there are two permanent weather systems of regional character that substantially contribute to this high frequency of northerly and southerly winds. Firstly, the combination of high barometric pressure over the Balkans with low pressure over the eastern Mediterranean causes the north winds, known as the 'Etesians', in the summer months (Meteorological Office 1965). Secondly, the local sea- and land-breeze mechanism is responsible for winds from the southern sector during the warm hours of the day in late spring and in summer (Prezerakos 1986). Another sea-breeze cell is established in the Mesogia Plain and gives rise to an airflow through the pass between the Hymettos and Penteli mountains. At that point, because of the vertical motion created by the opposing sea-breeze currents (south-west and north-east), some convective clouds appear that are occasionally significant (Clement 1989).

4. Rainfall data in the Greater Athens Area

The 24 rain-gauges selected for the present investigation belong to different Greek institutions: the previously mentioned MINOA station, ten stations of the Water and Sewage Corporation (WSC), six stations of the National Meteorological Service (NMS), five stations of the Ministry of Environment, Planning and Public Works (MEPPW), one station of the Vineyard Institute of the Ministry of Agriculture (VIMA) and one private station. The list of the stations used, together with their geographical coordinates and their elevations above mean sea level, is given in Table I, and their network distribution is shown in Fig. 2.

Since the objective of the present study was to determine the spatial distribution of rainfall the GAA, a major effort was made to take into account data from the maximum number of stations with continuous records for the period 1985–89. On the other hand, special care was given to avoid effects arising from improper exposure, change of exposure, instrumental failures or change of station site during the examined period. The representativeness of the 5-year period was also examined by comparing it with the climatological

Table I. Rainfall stations in the Greater Athens Area used in this study. See Fig. 2 for locations, and text for explanation of acronyms.

No.	Station	Institution	Longitude	Latitude	Height (m)
1	MINOA	MINOA	23° 43′E	37° 58′N	107
2	Filadelfia	NMS	23° 44′E	38° 02′N	136
3	Peireas	NMS	23° 38′E	37° 56′N	3
4	Helliniko	NMS	23° 44′E	37° 54′N	10
5	Eleysina	NMS	23° 33′E	38° 03′N	30
6	Megara	NMS	23° 21′E	38° 00′N	36
7	Egina	NMS	23° 26′E	37° 45′N	3
8	Vyronas	MEPPW	23° 45′E	37° 57′N	120
9	Nikaia	MEPPW	23° 39′E	37° 58′N	20
10	Halandri	MEPPW	23° 48′E	38° 02′N	180
11	Peristeri	MEPPW	23° 42′E	38° 01′N	60
12	Markopoulo	MEPPW	23° 56′E	37° 53′N	85
13	Anavyssos	Private	23° 57′E	37° 42′N	80
14	Lykovrysi	VIMA	23° 47′E	38° 04′N	220
15	Tatoi	WSC	23° 47′E	38° 06′N	237
16	Horio	WSC	23° 58′E	38° 09′N	60
17	Fragma	WSC	23° 54′E	38° 10′N	240
18	Stamata	WSC	23° 53′E	38° 08′N	370
19	Kapandriti	WSC	23° 53′E	38° 13′N	340
20	Varnavas	WSC	23° 55′E	38° 14′N	480
21	Kiourka	WSC	23° 50′E	38° 12′N	400
22	Katsimidi	WSC	23° 49′E	38° 11′N	570
23	Hani	WSC	23° 51′E	38° 08′N	260
24	Bogiati	WSC	23° 51′E	38° 08′N	350

data obtained from the longest rainfall time-series of MINOA.

In order to study the rainfall amounts in the different regions in the GAA (as defined in section 2), the rainfall data from the 24 stations were grouped into six categories for further analysis; the criterion for this grouping was mainly geographical. Because of the length of the Athens Basin, it was subdivided into the South and North Athens Basins. The height of each station above mean sea level was also taken into consideration in this division, as a relationship between station height and rainfall amount exists (Smith 1979).

The categories into which the GAA was divided were the following:

South Athens Basin (SAB) which includes six stations (MINOA, Peireas, Helliniko, Nikaia, Vyronas and Peristeri).

North Athens Basin (NAB) which includes four stations (Filadelfia, Halandri, Lykovrysi and Tatoi).

Thriassio Field which includes two stations (Eleysina and Megara).

Egina Island with its homonymous station.

Mesogia Plain with two stations (Markopoulo and Anavyssos).

Marathon Area which includes nine stations (Horio, Fragma, Stamata, Kapandriti, Varnavas, Kiourka, Katsimidi, Hani and Bogiati).

5. Results and discussion

5.1 Temporal variations of rainfall

The monthly values of rainfall in the six regions of the GAA for the period 1985–89 are shown in Fig. 3 and the corresponding monthly mean values for the same period are shown in Fig. 4. It is obvious, that the rainfall in the GAA presents a strong seasonal variation with wet winters and dry summers, as in the typical Mediterranean climate, which is a result mainly caused by the synoptic circulation explained before. The monthly values of rainfall vary greatly from month to month. Calculations from the long-term rainfall series of MINOA have shown that the correlation between pairs of months is very low, which has been attributed to the relative independence among the synoptic conditions characterizing the rainfall in each season (Katsoulis and Kambezidis 1989). It is important to note that 1989 was relatively dry, especially for the southern part of the GAA. In that year rainfall (150.6 mm) was the lowest measured at the MINOA station for this century. This effect is related to the general drought problem experienced recently (continuing during 1990) all over Greece, which has in particular created severe problems for the water resources of the city of Athens.

The correlation among the records from the different parts of the GAA is relatively high, and the corresponding

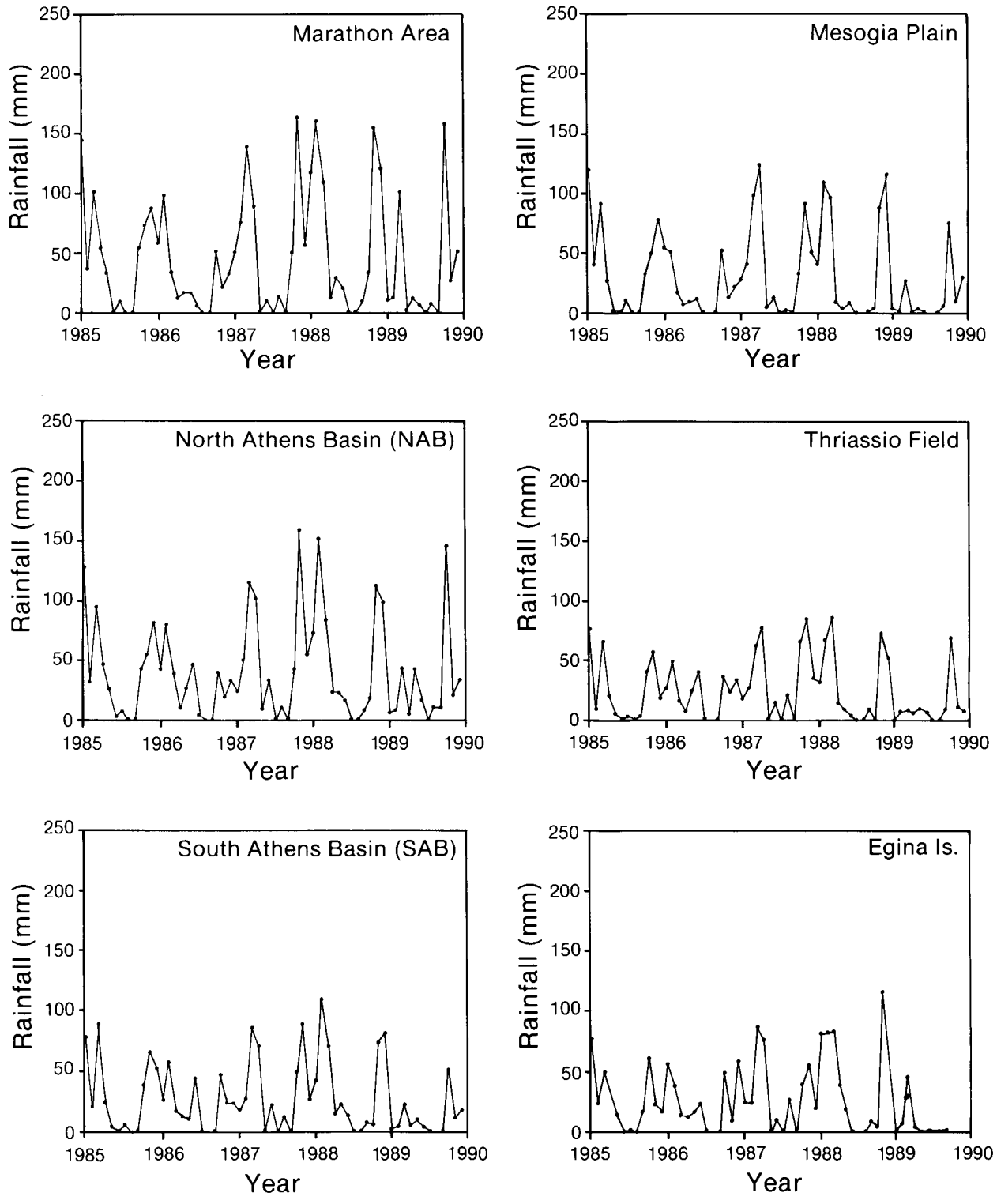

Figure 3. The monthly values of rainfall in the six regions of the Greater Athens Area for the period 1985–89.

coefficients are presented in Table II. The higher correlation coefficients are observed between the pairs of the SAB, NAB and Marathon Areas. This fact is explained by the coincidence of the geographically consecutive areas with the south-west to north-east alignment of the atmospheric circulation. The smaller correlation coefficient is observed when the area of Egina Island is considered. This may be attributed to the different behaviour of rainfall due to the airflow's divergence–convergence mechanism commonly observed in island regions.

The monthly mean variation of rainfall for the period 1985–89 in the six parts of the GAA, presented in Fig. 4, is characterized by a persistent and unexpected maximum in March for all groups of stations. At the end of the year the maximum rainfall appears in November. Consequently, the 5-year period presents a secondary minimum during winter. Katsoulis and Kambezidis (1989) have also

Table II. Correlation coefficients among the rainfall records in the Greater Athens Area. See Fig. 2 for locations of areas.

South Athens Basin (SAB)	1					
North Athens Basin (NAB)	0.949	1				
Mesogia	0.921	0.926	1			
Thriassio	0.934	0.888	0.884	1		
Marathon	0.904	0.949	0.914	0.841	1	
Egina	0.830	0.820	0.827	0.843	0.859	1
	SAB	NAB	Mesogia	Thriassio	Marathon	Egina

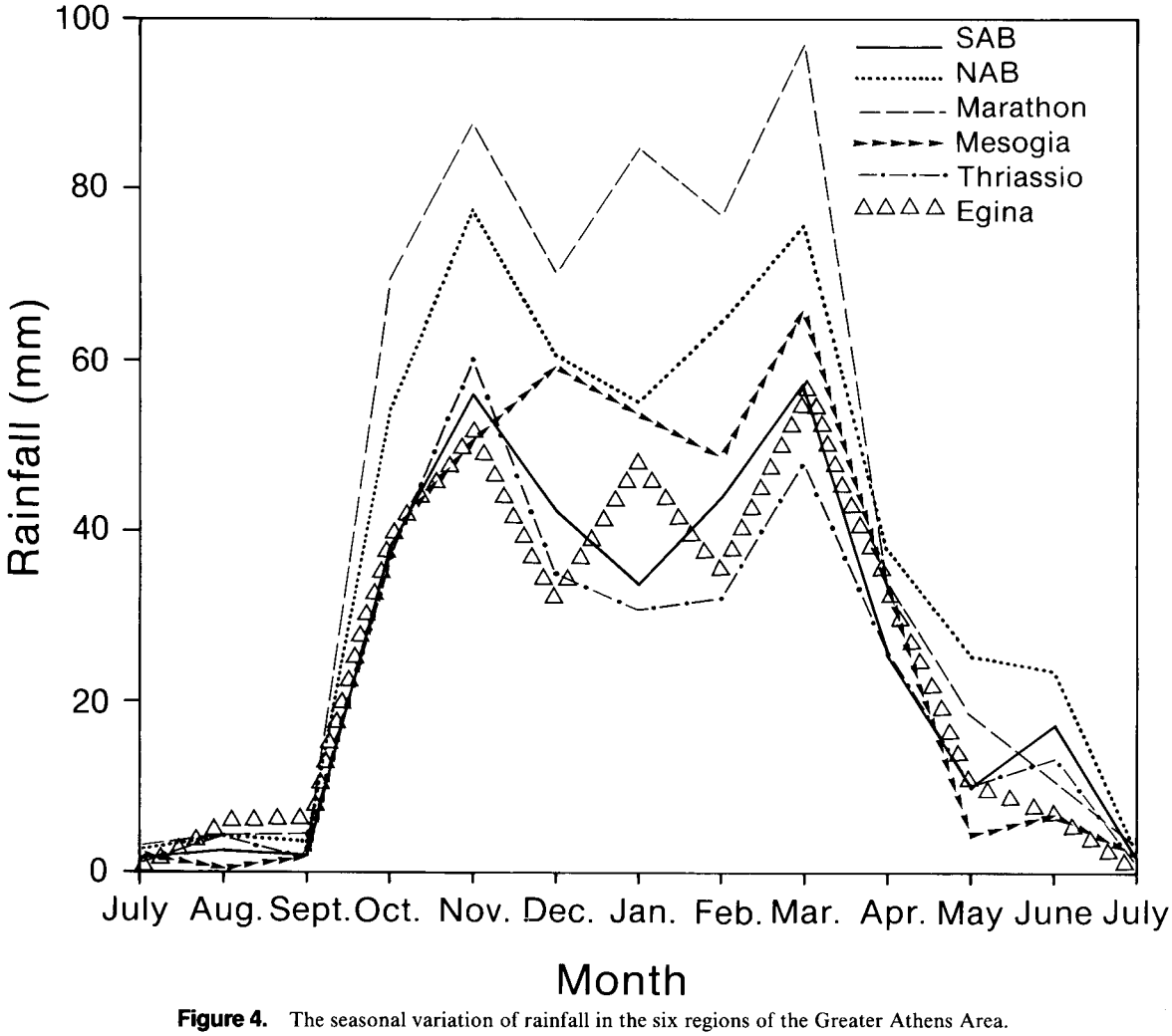

Figure 4. The seasonal variation of rainfall in the six regions of the Greater Athens Area.

observed during the most recent period (1951–85) at the MINOA station an increasing tendency of rainfall amount in the transitional seasons (which are the unstable part of the year), although at the same time a noteworthy significantly negative trend was found to characterize the annual rainfall amounts. They qualified this phenomenon as indicative of an urban effect (Changnon 1968, Goldreich and Manes 1979). The slightly increasing tendencies of rainfall amount are attributed to the urban heat-island effect and the surface roughness in the city, which both increase the turbulence and the atmospheric instability. A similar conclusion was also drawn by Goldreich and Manes (1979) for the Tel-Aviv urban area. In this respect, it is interesting to note that in the GAA the less pronounced decreases appear at the Marathon and Egina Areas which are the less urbanized.

In order to get more insight into the shift of the rainfall maximum towards March, the climatological data at the MINOA station for the periods 1891–1985, 1951–80 and 1980–89 along with the period of interest 1985–89 are plotted together in Fig. 5. The comparison shows that the March particularity appears also in the monthly mean variation of the last decade (1980–89). This result is likely to be of climatological interest.

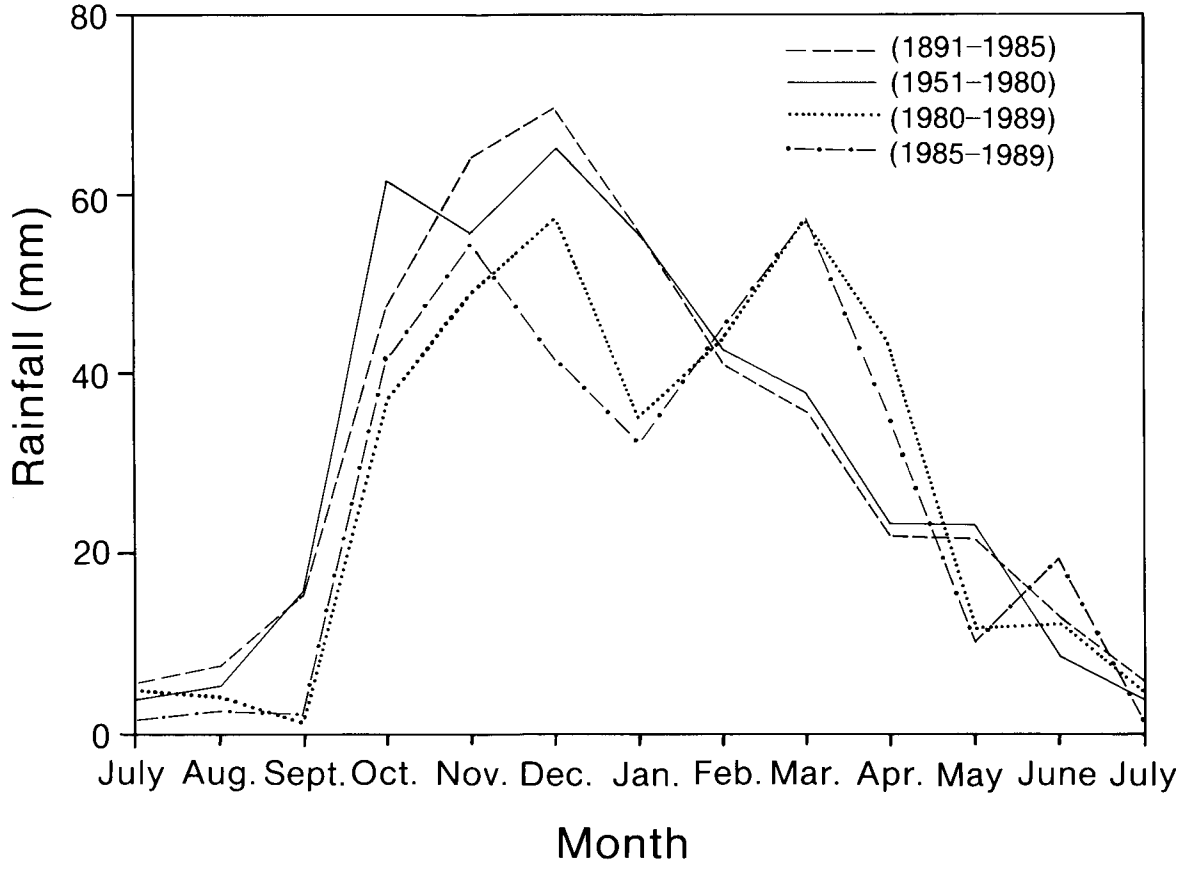

Figure 5. The seasonal variations of rainfall at the MINOA station (see Table I) for the periods 1891–1985, 1951–80, 1980–89 and 1985–89.

5.2 Rainfall variation with station height

As is well known, rainfall tends to increase with height and decreases with depth down in an isolated valley (Smith 1979). On very high mountains the rainfall increases up to a certain height (up to 2 km) and then decreases, because above this height the ascending air masses lose their water vapour content. The relationship between the average annual rainfall and the height of the station above mean sea level is in most cases linear. The scattering in the linear-regression representation is caused by the failure of the relationship to describe the upslope-rain to rain-shadow contrast, which is important for broad mountains. If the region under consideration has a consistent prevailing wind, this latter effect is well represented by the spatial distribution of annual rainfall.

In Table III, the average annual rainfall and the mean height of the stations for the six different areas in the GAA are presented. It is ascertained that rainfall increases with height. The maximum rainfall occurs in the hilly area around the Marathon lake. On the other hand, the minimum rainfall occurs in the south-west part of the GAA at the Thriassio Field and the Egina Island where the stations are very close to sea level.

In Fig. 6, the average annual rainfalls for the period 1985–89 at the 24 stations in the GAA have been plotted against the station heights. Although the station height used is not obtained by any averaging process considering the surrounding area (Goh and Lockwood 1974, Hill *et al.* 1981) the correlation is relatively high ($r = 0.826$), which indicates that variations of annual rainfall amounts account for 68% of the variance of the station height. The 32% uncorrelated variance of rainfall is attributed to the upslope-rain to rain-shadow contrast, as mentioned before. The linear-regression equation, obtained in Fig. 6, $R = 306.8 + 0.685H$ is valid for the GAA, where the rainfall R is measured in millimetres and the station height H in metres. The slope of the linear best fit suggests that annual rainfall amounts increase by 68.5 mm for each 100 m increase of the station height. The intercept of the linear best fit indicates that there is an annual rainfall of about 300 mm in the GAA for any stations with zero height.

The correlation between the monthly rainfall amounts and the station height presents a seasonal variation. The

Table III. Rainfall amounts at different regions of the Greater Athens Area. The areas are the same as in Table II.

Area	Number of stations	Average height (m)	Average annual rainfall (mm)
SAB	6	53	320.9
NAB	4	193	465.8
Mesogia	2	83	366.4
Thriassio	2	33	275.5
Egina	1	3	288.4
Marathon	9	341	557.2

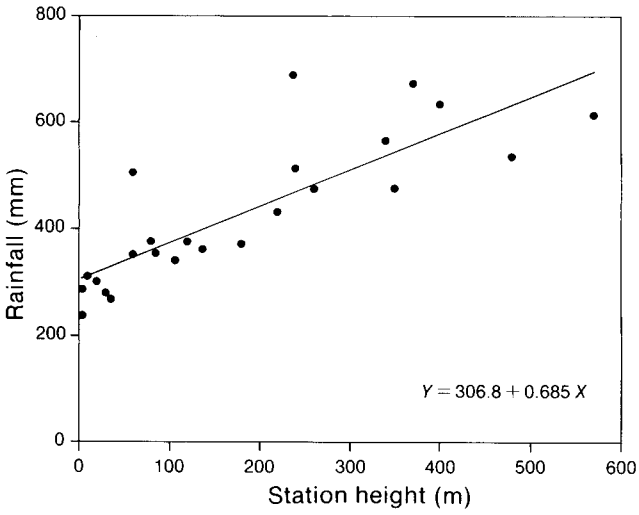

Figure 6. The average annual rainfall for the period 1985–89 versus station heights above mean sea level.

correlation coefficients are high for January (0.696) and October (0.789), but are low for April (0.271) and July (0.155). These results confirm that the frontal rainfall during the cold period of the year is strongly affected by the presence of mountains, while the thunderstorm activity during the warm period of the year is less affected by the local topography. The October maximum correlation coefficient calculated for the GAA is in accordance with Bergeron (1968, 1973). During the fall months, he found in Uppsala, Sweden, a remarkably strong dependence of rainfall on height — primarily caused by rain from stratified clouds.

5.3 Spatial variations of rainfall

The great spatial variability characterizing the rainfall in the GAA is not only attributed to the synoptic disturbances. Geographical and topographical factors, such as mountains, hills, plains, sea and islands in the GAA, produce microclimatic effects on the mesoscale circulations and significantly disturb the distribution of rainfall in the GAA. As a result, there will be as many different spatial rainfall distributions as there are days considered. Some degree of generalization is therefore essential, and consequently the spatial distribution of rainfall in the GAA is analysed on a monthly basis.

The average annual distribution of rainfall in the GAA for the 5-year period 1985–89 is shown in Fig. 7. The maximum rainfall occurs in the Marathon Area and more precisely on the south-east side of Mt Parnitha, while the minimum rainfall occurs in the south-west part of the GAA over the Salamina and Egina islands. A gradient is observed between inland and coastal areas along the south-west to north-east direction. The annual rainfall amounts double in the Marathon Area in comparison to the coastal areas. Repapis (personal communication) has also observed a similar gradient using earlier data from stations at SAB, NAB, Mesogia and Thriassio Areas. The rainfall gradient in the GAA is mainly attributed to the rain-bearing depressions

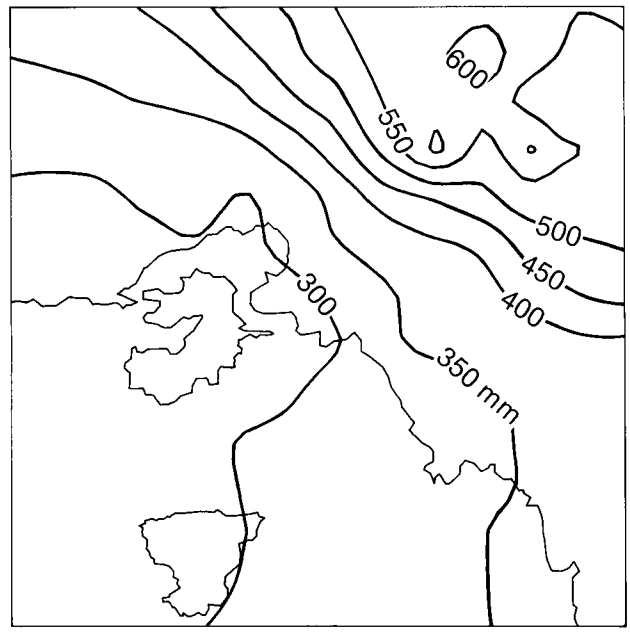

Figure 7. The average annual spatial distribution of rainfall in the Greater Athens Area for the period 1985–89.

moving from south-west to north-east over the Attika peninsula. The air masses are influenced by the presence of the surrounding sea which is warmer than the adjoining land during the cold period of the year. The passage from the sea to the land, together with the forced ascent due to topographic effects, are thought to be responsible for the gradient observed. Furthermore, superimposed on the above mechanisms, an additional effect seems to occur over the Marathon Area which explains the enhancement of the rainfall amounts measured in this area. Indeed, the hills and the small-scale mountains around the Marathon lake enhance rainfall by the so-called 'seeder-feeder' mechanism advanced by Bergeron (1965), in which raindrops from pre-existing (seeder) clouds aloft wash out small cloud droplets within low-level (feeder) clouds over the hills. According to field observations and theoretical studies (Bergeron 1968, 1973, Hill *et al.* 1981, Carruthers and Choularton 1983, Grabowski 1989), hills receive 40–100% more rain than the surrounding areas, while for convective-type rainfall, they appear to have negligible influence on the spatial rain distribution.

In order to analyse the seasonal aerial distribution of rainfall in the GAA, four months (January, April, July and October) considered as representative for the respective seasons are used. The spatial distribution for each month is shown in Fig. 8. The mean rainfall distribution for January and October present the same patterns as the annual one. But, in the January case, the gradient increases and the difference between the coastal area and the Marathon Area becomes more than three times bigger. During April, the rainfall pattern changes and the observed gradient becomes much less pronounced. Maximum amounts of rain fall on the

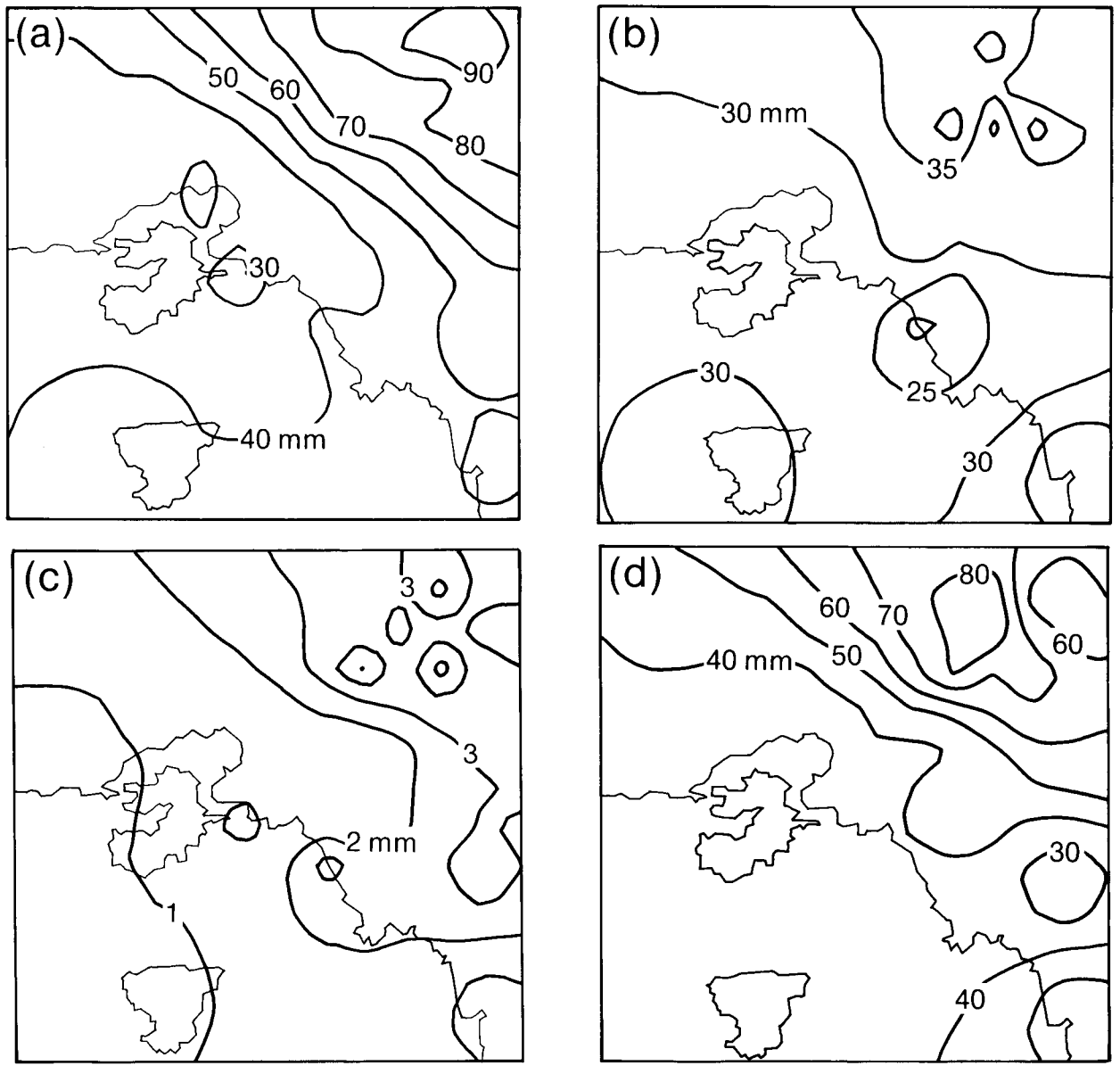

Figure 8. The spatial distribution of mean rainfall for the period 1985–89 in the Greater Athens Area for (a) January, (b) April, (c) July, and (d) October.

foot of Mt Parnitha and minimum at the south side of Mt Hymettos.

The July spatial distribution of rainfall is characterized by very low values (dry period of year). The influence of topography on rainfall distribution decreases, since for this season rainfall is only due to the local thunderstorm activity. High values of rainfall are observed in the Marathon Area and at Helliniko. The latter is in accordance with the work by Prezerakos (1989), who observed a greater number of thunderstorm days at Helliniko. He claimed that the thunderstorms start over the continental parts of Athens Basin and then develop towards the coasts of Saronikos Gulf.

6. Conclusions

The spatial distribution of rainfall in the GAA in Greece was examined in relation to the complex topography and the atmospheric circulation of this area. For this purpose, rainfall data from 24 stations for the 5-year period 1985–89 was analysed. This analysis revealed the following features:

(a) Although the rainfall in the GAA presents in general a seasonal variation with the maximum during the cold period of the year and a minimum during the warm period of the year, a secondary minimum is observed during winter in the examined period (appeared also in the last decade) intensified by the higher rainfall amounts measured in March.

(b) The annual rainfall amounts increase with height in the GAA by 68.5 mm for each 100 m increase of the station height above the mean sea level. A background annual rainfall of about 300 mm is considered as independent from the relief in the GAA. The correlation coefficient between the monthly mean

rainfall and the station height presents a seasonal variation with high values during the cold period of the year and low values during the warm period.

(c) The annual spatial distribution of rainfall presents a gradient between inland and coastal areas. As a result, rainfall at Marathon Area doubles in comparison with the coastal areas. The same distribution pattern is observed for January and October, while for April and July the gradient is much less pronounced due to the thunderstorm activity, which is less influenced by the local topography.

Acknowledgements

The authors are indebted to Pr. S.D. Papagiannakis for providing the rainfall data from his station at Anavyssos. Rainfall data for the GAA have been kindly provided by MINOA, NMS, WSC, MEPPW and VIMA.

References

Andreakos, C., Prezerakos, N.G. and Xirakis, P., 1984: Analysis of the air field in Athens. Final report of B6612/9. Athens, Ministry of Physical Planning, Housing and Environment.

Bartzis, J.G., Varvayanni, M., Catsaros, N., Konte, K. and Amanatidis, G.T., 1990: Wind field and dispersion modelling in complex terrain. Proceedings of the CEC seminar on methods and codes for assessing the off-site consequences of nuclear accidents. Athens, CEC Publications.

Bartzis, J.G., Venetsanos, A.G., Varvayanni, M., Catsaros, N. and Megaritou, A., 1991: ADREA-I, a transient three dimensional transport code for complex terrain and other applications. To be published in *Nuclear Technology*.

Bergeron, T., 1965: On the low level redistribution of atmospheric water caused by the orography. *In* Supplementary Proceedings of an International Conference on Cloud Physics. Tokyo.

—, 1968: Studies of orogenic effects on the areal fine structure of rainfall distribution. Uppsala Meteorological Institute, Report No. 6.

—, 1973: Mesometeorological studies of precipitation. Part V: Monthly rainfall in Uppsala field. Uppsala Meteorological Institute, Report No. 38.

Carruthers, D.J. and Choularton, T.W., 1983: A model of the seeder-feeder mechanism of orographic rain including stratification and wind-drift effects. *Q J R Meteorol Soc*, **109**, 575–588.

Changnon, S.A. (Jun.), 1968: The La Porte weather anomaly — fact or fiction? *Bull Am Meteorol Soc*, **49**, 4–11.

Clement, F., 1989: Air quality in the Greater Athens Area. II: Numerical simulations of the wind field. EUR 12245 EN, Joint Research Centre, Ispra, Italy, Commission of the European Communities.

Conrad, V., 1943: The climate of the Mediterranean Region. *Bull Am Meteorol Soc*, **24**, 4.

Goh, K.C. and Lockwood, J.G., 1974: An assessment of topographical controls on the distribution of rainfall in the central Pennines. *Meteorol Mag*, **103**, 275–287.

Goldreich, Y. and Manes, A., 1979: Urban effects on precipitation patterns in the greater Tel-Aviv area. *Arch Meteorol Geophys Bioklimatol*, **27b**, 213–224.

Grabowski, W.W., 1989: On the influence of small-scale topography on precipitation. *Q J R Meteorol Soc*, **115**, 633–650.

Hill, F.F., Browning, K.A. and Bader, M.J., 1981: Radar and raingauge observations of orographic rain over south Wales. *Q J R Meteorol Soc*, **107**, 643–670.

Housiadas, C., Amanatidis, G.T. and Bartzis, J.G., (1991): Prediction of orographically induced rainfall using Cartesian coordinates and a single prognostic equation for the water substance. To be printed in *Boundary-Layer Meteorology*.

Katsoulis, B.D. and Kambezidis, H.D., 1989: Analysis of the long-term precipitation series in Athens, Greece. *Clim Change*, **14**, 263–290.

Katsoulis, B.D., Tselepidaki, H. and Theoharatos, G., 1976: Characteristics of precipitation in Athens. *Bull Hell Meteorol Soc*, **VI, 2**, 1–19. (In Greek.)

Meteorological Office, 1962: Weather in the Mediterranean, Vols 1 and 2. London, HMSO.

—, 1965: Weather in the Mediterranean. London, HMSO.

Pissimanis, D., Karras, G., Notaridou, V. and Bartzis, J.G., 1989: Preliminary study on the flow field over Greece. *In* DEMO 89/1. Athens, NCSR Demokritos.

Prezerakos, N.G., 1986: Characteristics of the sea breeze in Attica, Greece. *Boundary-Layer Meteorol*, **36**, 245–266.

—, 1989: An investigation into the conditions in which air-mass thunderstorms occur in Athens. *Meteorol Mag*, **118**, 31–36.

Repapis, C.C., 1986: Temporal fluctuations of precipitation in Greece. *Riv Meteorol Aeronaut*, N 1–2, 19–25.

Smith, R.D., 1979: The influence of mountains on the atmosphere. *Adv Geophys*, **21**, 87–230.

Zerefos, C.S., Kosmas, G.B., Repapis, C.C. and Zampakas, J.D., 1977: Time series analysis of rain at Athens National Observatory during the century 1871–1970. Greece, University of Athens, Climatology Laboratory. (In Greek.)

551.509.543:625.7(410)

A comparison of UK road ice prediction models

J.E. Thornes and J. Shao
University of Birmingham

Summary

The performance of three models are compared and analyzed using a variety of statistical techniques.

1. Introduction

The climate of the British Isles in winter is usually characterized by the fluctuation of road surface temperatures around 0 °C together with a high humidity, which can induce the formation of ice or frost on road surfaces. This is obviously a serious potential hazard to all road users. There is a need for an accurate prediction of road surface conditions, to allow time for winter maintenance engineers to spread de-icing chemicals to prevent the formation of ice or frost or the accumulation of snow. Such phenomena also occur in many other countries with a cold and wet winter climate, such as northern and western Europe, Japan and North America. Three numerical road ice prediction models have been developed in the United Kingdom (Thornes 1984, Parmenter and Thornes 1986; Rayer 1987, Thompson 1988; Shao 1990) specifically for this purpose. Some others have also been developed outside the United Kingdom, such as the Swedish (Kempe 1990), French (Isaka *et al.* 1990), American SSI model (Stephenson 1988) and Finnish (Nysten 1980) models. Partly for commercial reasons, these other models are not available for comparison.

There have been few comparisons between the road ice prediction models using observed road surface temperature data (Thornes 1989), the COST-309 (1991) study merely comments on the availability of such models. This paper presents the results of a detailed comparison between the three UK road ice prediction models and also suggests a standard set of statistical parameters for such comparisons using:

(a) bias, standard deviation (SD) and r.m.s. error for overall, maximum and minimum temperatures,
(b) freezing time and duration, and
(c) forecast versus frost/no frost analysis.

Table I shows, for a matrix of values of forecast minus actual road surface temperature, the different measures of bias, r.m.s. error and SD that can be calculated for hourly and daily values.

For comparison, Chapman's Hill road weather outstation on the M5 motorway, West Midlands was chosen as the test site, due to the availability of roadside data and weather data from the University of Birmingham some 7 miles to the north-east. The three available models, i.e. the Thornes model (Thornes 1984), the Met. Office model (Rayer 1987, Thompson 1988) and the Icebreak model (Shao 1990) — developed on a 1987/88 winter database — are compared using a standard set of input data for the site taken from the winter of 1988/89. A comparison of the similarities and differences of the three models is given in Table II. The models also use different methods for the computation of the radiative and turbulent fluxes.

Table I. The derivation of hourly (H), daily (D) and overall (O), bias (B), r.m.s. error (R) and standard deviation (SD) for a matrix of values of forecast minus actual road surface temperatures.

	Hour of the day from noon (i)						
	1	2	.	.	.	I	
Day (n)							
1	X_{11}	X_{12}	.	.	.	X_{1I}	$B_D\ R_D\ SD_D$, e.g. $B_D = 1/I \sum_{i=1}^{I} X_{ni}$
2	X_{21}	X_{22}	.	.	.	X_{2I}	
.							
.							
.							
N	X_{N1}	X_{N2}	.	.	.	X_{NI}	
	$B_H\ R_H\ SD_H$, e.g. $B_H = 1/N \sum_{n=1}^{N} X_{ni}$						$B_O\ R_O\ SD_O$, e.g. $B_O = 1/N \sum_{n=1}^{N} B_{Dn}$

Table II. Brief description of similarities and differences between the Icebreak, Thornes and Met. Office models

	Icebreak	Thornes	Met. Office
1. Basic equation	Heat conduction	Energy balance	Heat conduction
2. Road temperature profile	Yes	No	Yes
3. Energy balance	Yes	Yes	Yes
4. Longitude	Yes	Yes	No
5. Sky view factor	Yes	No	No
6. Influence of traffic	Yes	No	No
7. Inputs*	T_a, T_d, W, C_a, C_t, R	T_a, T_d, W, C_a, C_t, R	T_a, T_d, W, C_a, C_t, C_l, R, P_r
8. Outputs**	T_s and wetness	T_s and wetness	T_s and wetness
9. Method of discreterization	Control volume	—	Finite difference
10. Derivation of forecast	Solving basic equation by fully implicit scheme	Searching for root of basic equation by iteration	Solving basic equation by explicit scheme

* T_a = air temperature; R_d = dew-point; W = wind speed; C_a = total cloud amount; C_t = dominant cloud type; C_l = low cloud amount; R = rain period; P_r = previous day's road temperature profile.
** T_s = road surface temperature.

2. Description of input data

All three models are run on a 24-hour cycle, projecting forward the measured noon road surface temperature. The model inputs are similar for all three models and are composed of six elementary meteorological variables: air temperature, dew-point, wind speed, total cloud amount, cloud type and precipitation. Cloud type is assigned 1 for low, 2 for medium and 3 for high cloud. Precipitation is represented with 0 for no rain, 1 for light rain and 2 for moderate or heavy continuous rain. For the Met. Office model, low-cloud amount is also needed. For comparison purposes the mean values over a 3-hourly interval are used. Besides the meteorological variables, road surface and depth (0.30–0.45 m) temperatures at noon are required by all three models.

To give an objective comparison, the models are run against each other in two different ways. Firstly, actual data measured at the roadside are used for the input data to produce a retrospective prognosis (RSP) — sometimes called a perfect prognosis. This enables the internal errors of the model schemes (physical and mathematical approximations) to be compared, eliminating errors related to forecast input. The input for the RSP consists of 95 days of data from the winter of 1988/89. Air temperature, dew-point and wind speed are taken from the measurements of the instruments mounted in and on roadside screens at a non-standard height of 2.0 m (for temperatures) and 3.0 m (for wind speed). Cloud data and rainfall intensity and duration are derived from the observations of the nearby weather station at the University of Birmingham.

Secondly, to assess the size of errors due to model interior shortcomings plus forecast input errors, the models are compared using real-time input data — i.e. real-time prediction (RTP). The real-time input was produced by Birmingham Weather Centre at Elmdon for Hereford and Worcester County Council as part of an 'Open Road' commercial contract. For the purpose of this comparison the days selected are those when the forecast input was issued around noon and not updated later, which gives a data set of 65 days.

Each model is run at an initial time of 1200 UTC and compared with hourly measurements of road surface temperature obtained from a road surface sensor in the fast lane of the motorway. The accuracy of this sensor is approximately ± 0.5 °C, and the calibration was checked twice during the winter period considered.

3. Comparative results for RSP

3.1 Diurnal and overall analysis of RSP

The hourly differences of predicted and measured road surface temperatures are first calculated for the Thornes, Met. Office and Icebreak models with the actual observed inputs. The biases and SDs for each hour are shown in Figs 1–3. The results can be expressed as follows:

(a) The Met. Office model has a consistent cool bias that is more than −0.9 °C for every hour except 1300 UTC and is as low as −1.5 °C in the evening and morning. The Thornes predictions are less cool, its bias reduces in the late evening and early morning (2100–0700 UTC), but increases notably in the late morning. The Icebreak model has a relatively small bias that is the closest of the three to zero.

(b) For hourly SDs, all three models have smaller values at night. This can be explained by a simpler parametrization procedure at night as the main external forcing term — solar radiation (which is difficult to model due to the unknown shadowing effect of broken cloud) — is excluded, and the models can cope with the surface energy balance better. The

Thornes model has the largest SD, more than 1 °C during the day and night, whilst the Met. Office model and the Icebreak model have less than 1 °C SDs (as low as 0.7 °C for the Met. Office model and 0.6 °C for the Icebreak model) at night.

The overall bias, SD and r.m.s. error of model predictions were calculated by averaging the hourly errors and are shown in Table III. For the purpose of comparison, it should be noted that a bias expresses the mean status of prediction errors, such that a negative bias means that the model predictions are too cold. The SD indicates the range of variance of the errors and the r.m.s. error is referred to as a measure of the total errors. A good model is expected to have a small absolute bias and a small SD or small r.m.s. From Table III and Figs 1–3 it can be seen that, in the prediction of overall temperatures, the Icebreak model is of the highest accuracy. The Thornes model has a larger standard deviation and thus differs more from actual values. The Met. Office model tends to be much cooler than reality and has the largest r.m.s. value. For winter maintenance applications a small negative bias is preferable — erring on the side of caution, i.e. some de-icing chemicals wasted but fewer potential accidents (Thornes 1989). Obviously, small values of SD and r.m.s. error are also required.

3.2 Minima and time of freezing of RSP

One of the important aspects of model comparison is also to look at the minimum temperature prediction and the time of start and duration of freezing. The daily predicted minimum road surface temperature for each model has been compared with the observed minima to yield the mean of the difference of minimum temperature, r.m.s., SD and frequency distribution of the difference. When both predicted and measured temperatures fall to, or below, 0 °C ($T_s \leqslant 0$ °C), the time and duration are compared and their differences calculated. Table IV gives a comparison for the three models in the differences of the minima, start time and duration of freezing.

From Table IV it is interesting to note that in the prediction of minimum surface temperature, the Thornes model has a small bias with a large SD and the Met. Office model has a smaller SD with a much larger bias. The Icebreak model has both the smallest bias and SD. In comparing freezing time and duration, the prediction of the Thornes model is 37 minutes later than the actual freezing time and 19 minutes ahead of actual surface temperature rising above 0 °C. The Met. Office model tends to issue an icing warning almost an hour early, and the warning lasts 2 hours longer than the actual period of freezing. Compared with the Thornes and Met. Office models, the Icebreak model has the smallest errors in predicting freezing time (30 minutes early).

The frequency distributions of the difference between actual and predicted minimum temperatures for the

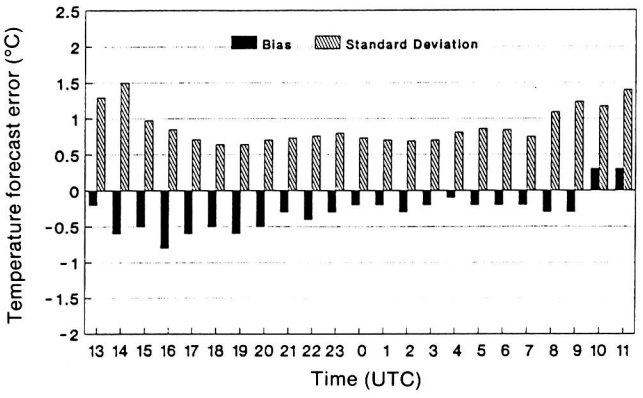

Figure 1. Hourly error analysis of retrospective prognosis for the Icebreak model (Chapman's Hill, winter 1988/89, 95 days).

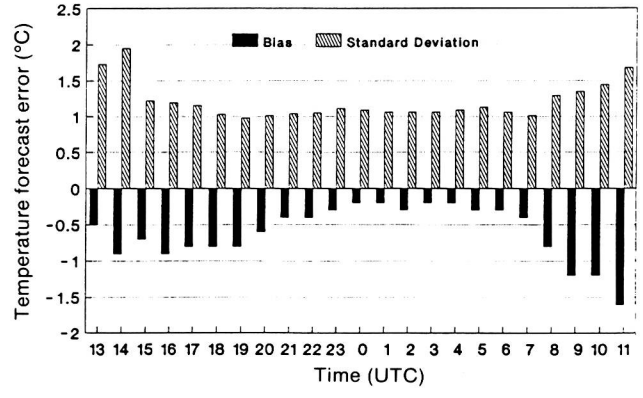

Figure 2. As Fig. 1 but for the Thornes model.

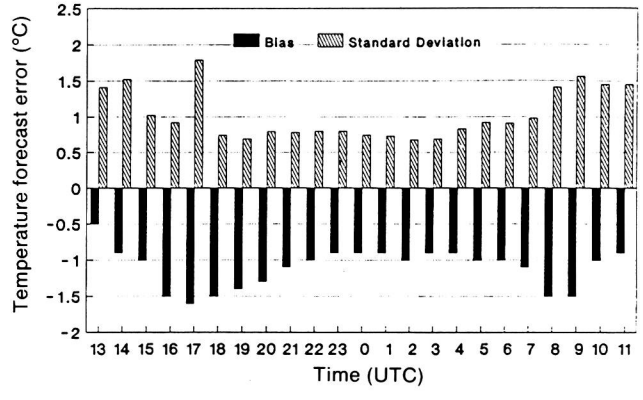

Figure 3. As Fig. 1 but for the Met. Office model.

Table III. Overall errors of retrospective predictions for model comparison (Chapman's Hill, winter 1988/89, 95 days) calculated from the average hourly errors

	Icebreak	Thornes	Met. Office
No. of hours*	2164	2164	2164
Bias	−0.29	−0.61	−1.14
SD	0.956	1.284	1.048
r.m.s.	1.000	1.418	1.543

* Note that 2164 hours of data were available for analysis out of 2280 (94.9%) owing to data loss from road sensor.

Table IV. Differences of predicted and measured road surface temperature minima (°C), freezing start time and duration (min.) for model comparison (Chapman's Hill, winter 1988/89, 95 days)

	Icebreak	Thornes	Met. Office
Minima:			
Number	95	95	95
Bias	−0.11	−0.17	−0.92
SD	0.757	1.022	0.786
Freezing:			
Number	19	16	19
Start time*	30	−37	57
Duration**	37	−19	123

* A positive number indicates that the road surface temperature was predicted to fall to 0 °C before it actually did.

** A positive number indicates that the duration of time at or below 0 °C was predicted to be too long.

models are shown in Figs 4–6. For an accuracy in absolute error in the prediction of minimum road surface temperature of ± 0.5 °C, 57.9% of the Icebreak model, 42.1% of the Thornes model and only 25.3% of the Met. Office model are found. Most of the absolute prediction errors of the Icebreak model (87.3%) and Thornes model (76.3%) are less than 1.0 °C;for the Met. Office model predictions 55.5% are of this accuracy.

An analysis of 'frost' (defined simply as road surface temperature falling to 0 °C or below) or 'no frost' forecasts against 'frost' or 'no frost' occurring (forecast/actual) has also been made and the results are given in Table V. As classified by Thornes (1989), the potential consequences of an erroneous forecast are:

Type 1 error (T1): Forecast 'no frost', actual 'frost' — potential for accidents,

Type 2 error (T2): Forecast 'frost', actual 'no frost' — potential for wasting de-icing chemicals.

Table V shows that for the 95 nights (with 21 frosts), T1 is the highest for the Thornes model, while T2 is the highest for the Met. Office model.

3.3 Maximum temperature of RSP

An accurate prediction of maximum road surface temperature (usually afternoon temperatures) is another important aspect of a successful model. It acts as to convince highway engineers of the model accuracy, for the engineers compare model prediction with sensor measurements in the afternoon, and may believe that an incorrect prediction of maxima will lead to a wrong prediction of minima in the night-time.

The analysis of model retrospective prognoses for the maximum temperature is given in Table VI. Both the Thornes model and the Met. Office model give much cooler bias than the Icebreak model, and the Thornes model has the largest SD. It is seen from the table that the Icebreak model has significantly improved the prediction of maximum temperature.

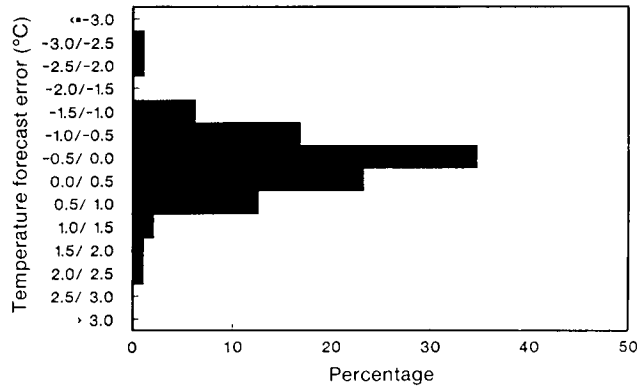

Figure 4. Distribution of the difference of forecast minus actual minimum temperature in retrospective use of the Icebreak model (Chapman's Hill, winter 1988/89, 95 days).

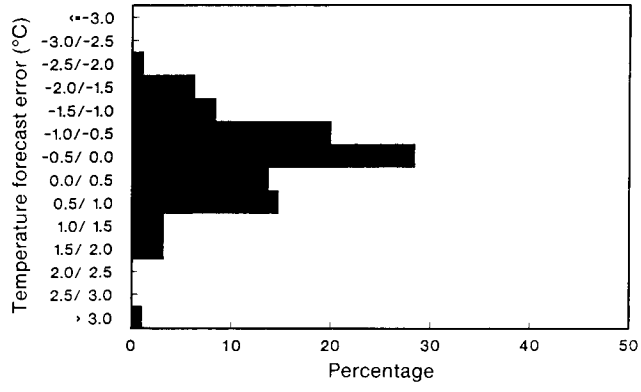

Figure 5. As Fig. 4 but for the Thornes model.

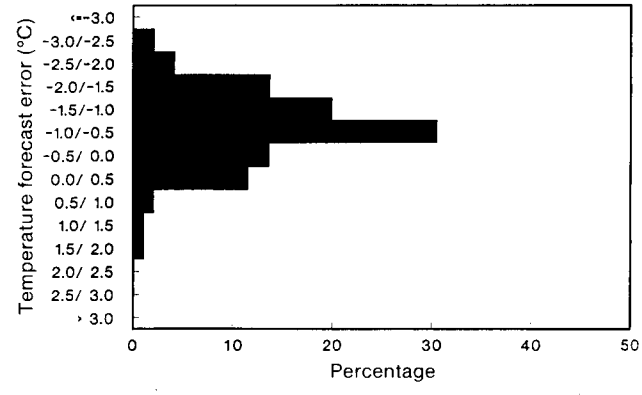

Figure 6. As Fig. 4 but for the Met. Office model.

4. Comparative results using 'realistic' Open Road input data

To see what the potential accuracy of model prediction is in view of the fact that perfect predicted data are never available, the three models were run using the 'realistic' input data used by the Birmingham Weather Centre for the nights concerned. This gives an estimate of the scale of model prediction errors in routine operation. Note that although only 65 days were

Table V. Model comparison of frost forecast accuracy with actual roadside input (Chapman's Hill, winter 1988/89, 95 days). (See text for explanation of T1 and T2)

Forecast/actual	Icebreak		Thornes		Met. Office	
	No.	%	No.	%	No.	%
No frost/no frost	73/74	98.6	74/74	100.0	69/74	93.2
Frost/no frost T2	1/74	1.4	0/74	0.0	5/74	6.8
Frost/frost	19/21	90.5	16/21	76.2	19/21	90.5
No frost/frost T1	2/21	9.5	5/21	23.8	2/21	9.5
Overall	92/95	96.8	90/95	94.7	88/95	92.6

Table VI. Model comparison for road surface temperature maxima prediction (Chapman's Hill, winter 1988/89, 95 days)

	Icebreak	Thornes	Met. Office
Number	95	95	95
Bias	−0.56	−1.22	−1.24
SD	1.597	1.972	1.571

selected for this analysis, the results for the retrospective model runs given in Table VII are very similar to those discussed in section 3.

4.1 Errors in predicted input

There is a need to investigate how accurate was the forecast input data used in the real-time prediction. The mean and maximum differences, SD and r.m.s. of the differences between real-time input (forecast) and retrospective input (actual) for screen air temperature and dew-point, wind speed, cloud amount, cloud type and rainfall for the 65 days are given in Table VIII. The differences are calculated from the values pertaining at 3-hourly intervals. It should be noted that there are height differences between actual (2.0 m) and forecast (1.2 m) air temperatures and dew-points, and actual (3.0 m) and forecast (10.0 m) wind speeds.

It is seen from the table that the most reliable variables predicted in real-time input seem to be air temperature and cloud type. All the others have a large difference. The difference in wind speed may be partly explained by the difference in the height where wind speed was derived, but this can only be surmised.

4.2 Comparison of model potential accuracy

The purpose of this exercise is to compare the size of errors due to model interior shortcomings (as discussed in section 3 for perfect predictions) with those due to forecast input errors. The comparison of retrospective prognoses and real-time predictions (of the same 65

Table VII. Model comparison of retrospective (RSP) and 'real-time' (RTP) runs (Chapman's Hill, winter 1988/89, 95 days)

	Icebreak		Thornes		Met. Office	
	RSP	RTP	RSP	RTP	RSP	RTP
No. of hours*	1480	1480	1480	1480	1480	1480
Overall:						
Bias (°C)	−0.33	−0.10	−0.61	−0.17	−1.15	−0.42
SD (°C)	0.75	1.14	0.97	1.12	0.81	1.02
r.m.s. (°C)	0.93	1.43	1.31	1.42	1.45	1.28
Maximum:						
Bias (°C)	−0.56	−0.16	−1.10	−0.73	−1.13	−0.78
SD (°C)	1.58	1.63	1.96	1.87	1.60	1.52
Minimum:						
Bias (°C)	−0.17	−0.38	−0.19	−0.11	−0.94	−0.26
SD (°C)	0.69	1.64	1.10	1.48	0.85	1.32
Time of freezing:						
Freezing (nights)	17	17	15	15	17	16
Start (minutes)	37	64	−28	52	46	−49
Duration (minutes)	52	56	−12	68	103	0

* 1480 hours out of 1560 possible (95% availability)

Table VIII. Comparison of meteorological variables between real-time input and actual roadside input (Chapman's Hill, winter 1988/89, 65 days)

	Realistic with actual		
	Mean error	SD	Maximum error
Air temperature (°C)	0.07	1.534	5.50
Dew-point (°C)	0.44	1.710	5.90
Wind speed (knots)	2.75	3.860	17.00
Cloud amount* (oktas)	−0.43	2.236	8.00
Cloud type* (1–3)**	−0.19	0.748	2.00
Rainfall* (0–2)**	−0.53	0.794	1.00

* Although these are discrete rather than continuous variables, the analysis has still been done for comparison.
** See text for explanation.

days) for the three models is shown in Table VII. Note that the days chosen for this analysis were the 65 occasions when no update was issued, and hence the original noon forecast was considered good, and weather conditions did not change significantly from the forecast.

In terms of overall RTP errors, all three models have a negative bias and the Met. Office model is the coldest. Their SDs and r.m.s. errors are not much different. For maximum temperature, the Icebreak model is marginally colder than actual maximum (−0.16 °C) with SD of 1.63 °C. The Thornes model and Met. Office model are cooler. In the real-time prediction of minimum temperature, the Icebreak model and Thornes model tend to issue a freezing warning nearly an hour earlier than actual freezing, while the Met. Office model has a lag of 49 minutes in predicting the start of freezing. The Met. Office model has an error of zero in the prediction of duration of freezing conditions.

The results of forecast/actual frost analysis for the realistic prediction is listed in Table IX. It can be seen from the table that the overall accuracy of the three model is similar.

Comparing the ten left columns with the ten right columns in Table VII for each model, the Icebreak (7/10) and Thornes (6/10) models show an improvement with retrospective actual inputs, while the Met. Office (3/10) model shows little improvement. This suggests that the forecasters at Birmingham Weather Centre were varying the inputs to produce better results, as discussed further below. For the Icebreak model, the overall mean bias and maximum temperature bias of RSP are a little cooler than those of RTP; significant improvements of RSP are seen in the reduction of r.m.s. and SD values of overall and minimum temperatures. It is clear that with actual input, the model has improved its overall and minimum predictions, and freezing time. But it shows no improvement in the prediction of maximum temperature and freezing time over real-time running.

Compared with real-time predictions, the Thornes model shows an improvement in the prediction of overall and minimum temperature and freezing time with actual roadside input, while the Met. Office model has cooler predictions using perfect prognosis.

Looking at the overall errors, it can be seen that the SD of the Icebreak model is reduced from 1.14 to 0.75 using the perfect prognosis, a reduction of 34%. For the Thornes model the percentage reduction is about 13%, and the Met. Office model about 21%. The Met. Office model shows little potential for improvement using accurate or actual input in terms of both bias and r.m.s. error however. It is notable that the input from the weather forecasters significantly improved the output of the Met. Office model.

5. Discussion and conclusion

Although it is indicated in the previous section that the Icebreak model and Thornes model achieve improvements with actual roadside input, perfect prognosis for the Met. Office model is not superior to realistic prediction — this requires further investigation.

The first question is whether the difference of temperature and wind speed height between actual (2.0 and 3.0 m) and forecast (1.2 and 10.0 m) input can be considered as a significant contributing factor to the abnormal results of the Met. Office model. The difference of temperature height is about 0.8 m. It is reasonable to believe that this difference of temperature height can be ignored because the near-ground layer over the road is such a well-mixed layer that no big difference of vertical temperature should exist within so small a vertical distance, except on exceptional nights.

The difference in wind speed height is relatively large. Because of the inaccuracy of interpolation for a wind speed profile, roadside wind speed was not extrapolated to 10 m height in retrospective prognoses. By the same consideration of a well-mixed layer, however, the difference of wind speed due to the difference in height is not expected to be significant to the results, as sensitivity analysis shows that wind speed has a small influence on model output (Shao 1990). Therefore it can be concluded that the results in the model comparison are reliable.

A probable explanation for the abnormal results of the Met. Office model is that the model has been used operationally for 2 years and the local forecasters at Birmingham Weather Centre have become familiar with optimizing model output by varying model input.

Farmer and Tonkinson (1989) have undertaken a verification of the Met. Office model by comparing the results of perfect prognoses against actual road surface sensor (fast lane Chapman's Hill) measurements in the winter of 1988/89. Their perfect prognoses were made using actual roadside observations and airfield observation from Birmingham Airport. Their results are compatible with those derived here. The results all show a cool bias of the Met. Office model predictions.

Table IX. Model comparison of frost forecast accuracy with realistic Open Road input (Chapman's Hill, winter 1988/89, 65 days). (See text for explanation of T1 and T2)

Forecast/actual	Icebreak		Thornes		Met. Office	
	No.	%	No.	%	No.	%
No frost/no frost	45/47	95.7	47/47	100.0	45/47	95.7
Frost/no frost T2	2/47	4.3	0/47	0.0	2/47	4.3
Frost/frost	17/18	94.4	15/18	83.3	16/18	88.9
No frost/frost T1	1/18	5.6	3/18	16.7	2/18	11.1
Overall	62/65	95.4	62/65	95.4	61/65	93.8

By comparing bias, SD and r.m.s. error in a retrospective analysis, we believe that we have shown that the Icebreak model provides improved accuracy in predictions of maximum and minimum road surface temperature prediction, such as in the prediction of maximum, and frost frequency. The predictions of the Thornes model have a larger variance, and the predictions of the Met. Office model are too cold.

The predictions of the Icebreak model can be further improved with more accurate input, such as for wind speed and cloud. The Thornes model is of smaller potential to improve its predictions, and the Met. Office model has no such potential unless the negative bias is removed and the forecasters do not subjectively alter the inputs.

The results presented here are restricted by the use of a single test site, and research is now continuing for a selection of sites across the United Kingdom.

Acknowledgements

The authors wish to thank the following for assistance with this work: P. Buchanan and S. Manstone of the Met. Office, and J. Kings, J. Hales and R. Johnson of the University of Birmingham Weather Service for their generosity in providing all the data required. This work was made possible by grants from Vaisala TMI, the British Council and the Strategic Highway Research Program.

References

COST-309, 1991: Final report (In press).

Farmer, S.F. and Tonkinson, P.J., 1989: Road surface temperature model verification using input data from airfields, roadside sites and the mesoscale model. (Unpublished, copy available in the National Meteorological Library, Bracknell.)

Isaka, H. *et al.*, 1990: Prediction of road surface temperature. *In* Proceedings of the 5th International Road Weather Conference, Tromsø, 13 March 1990. Standing International Road Weather Commission.

Kempe, C., 1990: An estimation of the value of special weather forecasts in a pilot project for road authorities in Sweden. *In* Proceedings of the Technical Conference on Economic and Social Benefits of Meteorological and Hydrological Services, Geneva, 26–30 March 1990. World Meteorological Organization.

Nysten, E., 1980: Determination and forecasting of road surface temperature in the COST-30 automatic road station (CARS). (Unpublished, copy available in the National Meteorological Library, Bracknell.)

Parmenter, B. and Thornes, J.E., 1986: The use of a computer model to predict the formation of ice on road surfaces. Research Report RR71. Crowthorne, Transport and Road Research Laboratory.

Rayer, P.J., 1987: The Meteorological Office forecast road surface temperature model. *Meteorol Mag*, **116**, 180–191.

Shao, J., 1990: A winter road surface temperature prediction model with comparison to others. (Ph.D. thesis, University of Birmingham.)

Stephenson, T.E., 1988: Wisconsin's winter weather system. *In* Proceedings of the 4th International Conference on Weather and Road Safety, Florence, 8–10 November 1988. Standing International Road Weather Commission.

Thompson, N., 1988: The Meteorological Office road surface temperature prediction model. *In* Proceedings of the 4th International Conference on Weather and Road Safety, Florence, 8–10 November 1988. Standing International Road Weather Commission.

Thornes, J.E., 1984: The prediction of ice formation on motorways. (Ph.D. thesis, University of Birmingham.)

—, 1989: A preliminary performance and benefit analysis of the UK national road ice prediction system. *Meteorol Mag*, **118**, 93–99.

Satellite and radar photographs — 11 January 1991 at 0300 and 0316 UTC

On 11 January 1991 a frontal band of cloud (F–F–F in Fig. 1) was slow-moving, lying across northern France and the south-east coast of England. The eastern Atlantic was awash with vortices. In particular, cold air comma clouds (labelled A, B, C, D in Fig. 1), revealing enhanced convection, were running north-east just north of the frontal band. These brought thunderstorms with hail to southern counties of England and Wales during the day.

Comma A had induced a shallow wave on the front, at 0300 UTC near Luxembourg (see Fig. 1 inset). Comma B had a well-developed head of cirrus outflow and the

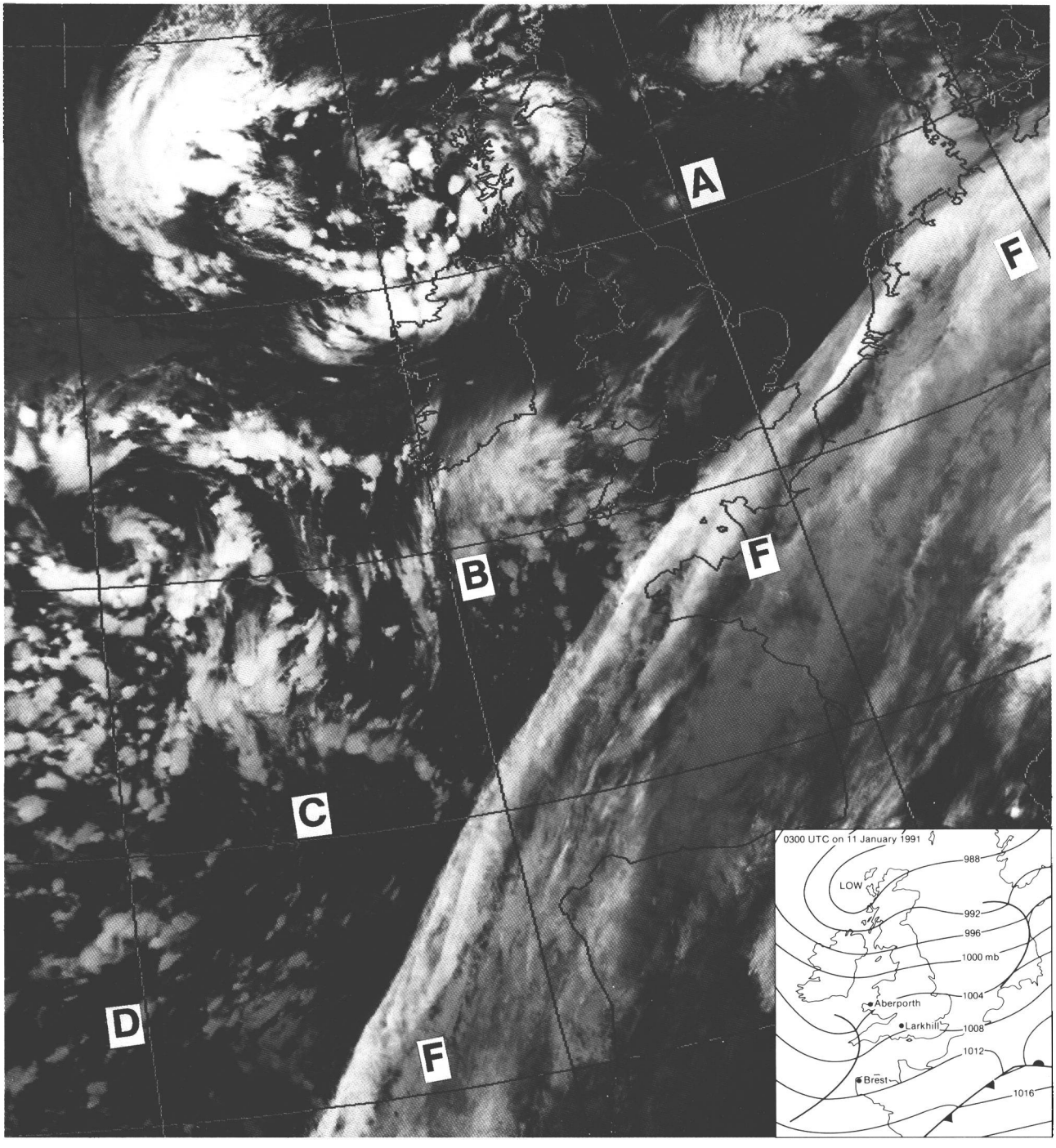

Photograph by courtesy of University of Dundee

Figure 1. NOAA-11 Channel 4 (infra-red) satellite picture at 0316 UTC on 11 January 1991. F–F–F is a slow-moving frontal band of cloud. A, B, C, D are four of the many vortices covering the Atlantic. The surface analysis for 0300 UTC is inset.

convection in the tail of the comma can be clearly seen beneath the frontal cloud to the west of Brest in Fig. 2.

The COST-73 satellite/radar composite for 0300 UTC (Fig. 3) shows the line of convective precipitation in the tail of the comma. Unfortunately the picture is complicated by previous storms to the north of Brittany. At 0600 UTC (Fig. 4) the radar picture is clearer, with the line of showers and thunderstorms extending well south over Brittany beneath the frontal cloud.

Radiosonde ascents show the air over England and Wales was unstable to around 400 mb — Larkhill (03743) is typical of this air (Fig. 5). Convective tops over Brittany were limited to 600 mb.

The orientation of certain cloud patterns is determined by the windflow relative to a moving system, rather than the actual winds reported, so it is useful to examine the relative flow to clarify the dynamical interpretation of the imagery. The relative wind is found by vectorially subtracting the system velocity (for comma B this was 245° 35 kn) from the actual winds. Plotted winds in Fig. 2 show the relative winds at 400 mb from radiosonde stations, plotted at appropriate positions relative to the

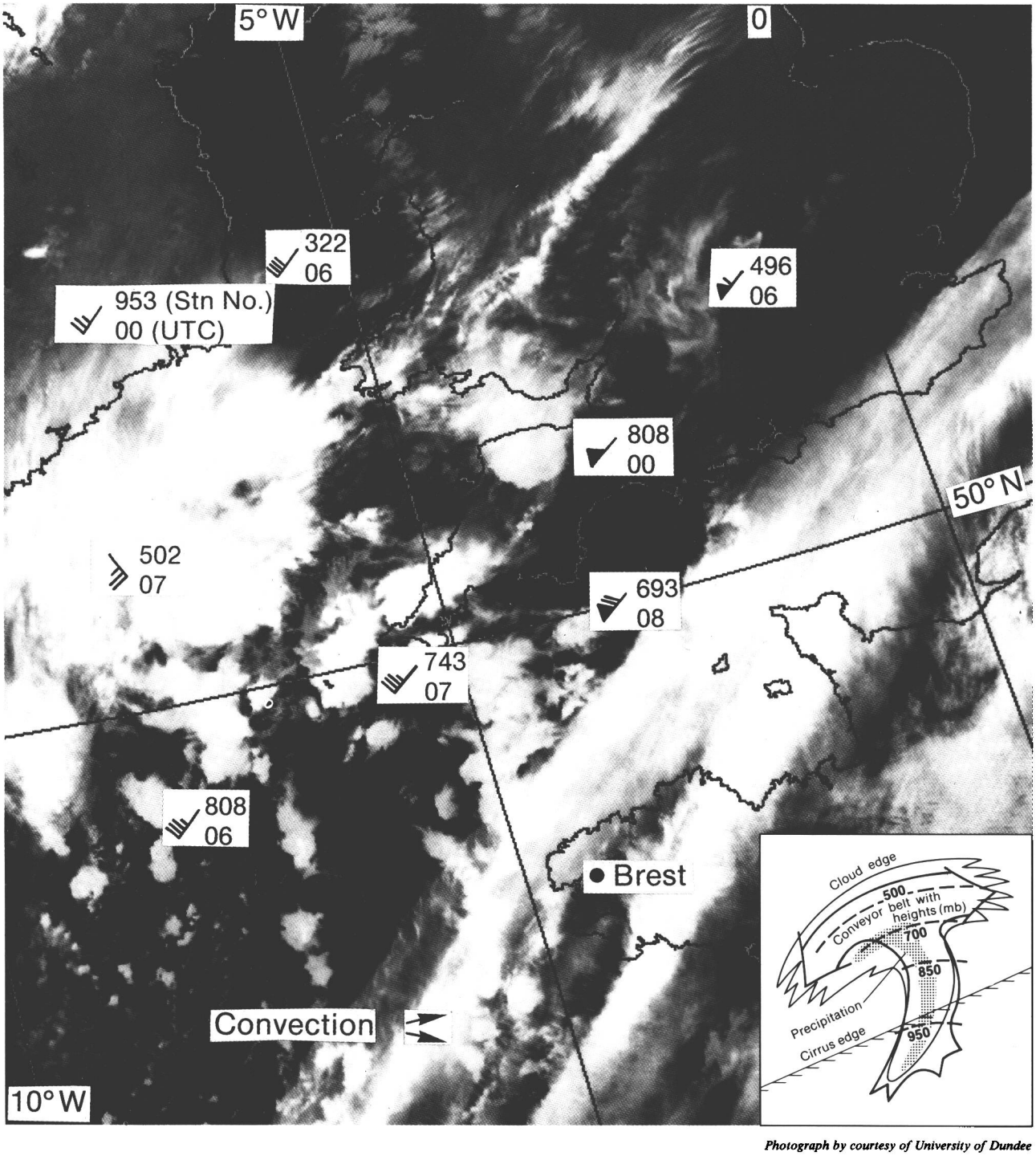

Photograph by courtesy of University of Dundee

Figure 2. As Fig. 1 but Channel 3. For explanation of wind plots and insert see text.

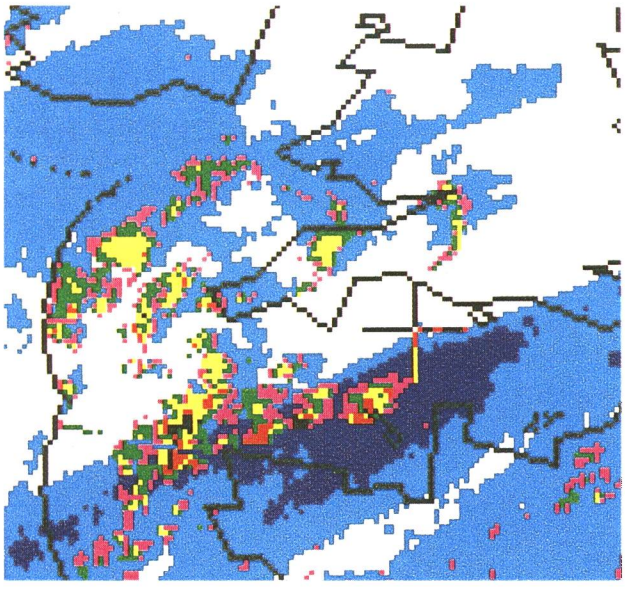

Figure 3. COST-73 satellite and radar image for 0300 UTC on 11 January 1991. Light blue represents cloud tops with temperatures between −15 and −45 °C and dark blue < −45 °C. Rainfall intensities (mm h^{-1}) are shown as follows: pink < 1, green 1–3, yellow 3–10, red 10–30. Coastlines, national boundaries and the limits of radar coverage are shown in black.

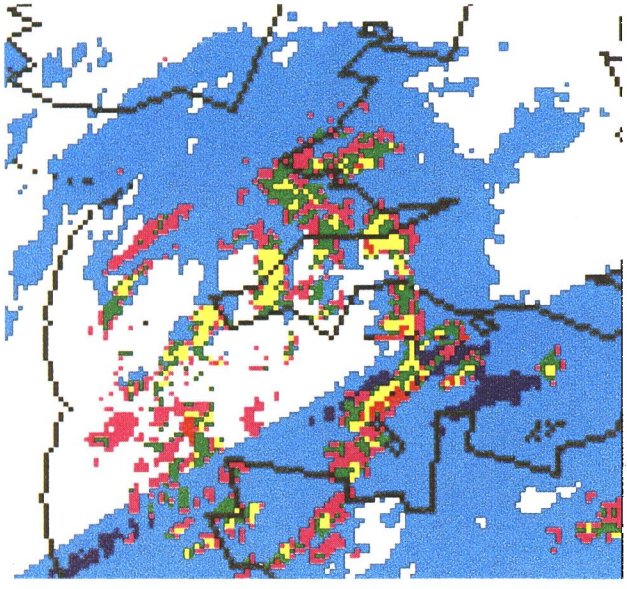

Figure 4. As Fig. 3 but for 0600 UTC.

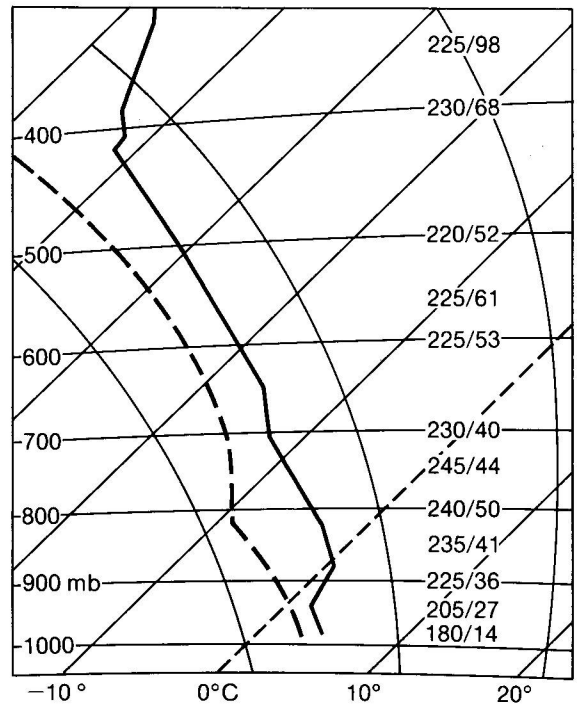

Figure 5. Tephigram for Larkhill (03743) at 0700 UTC on 11 January 1991.

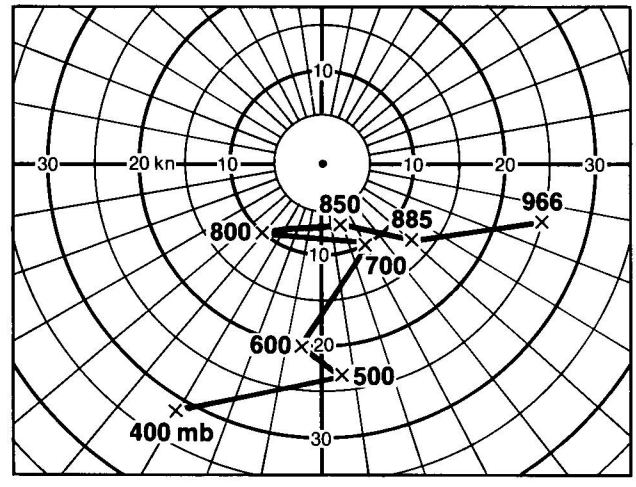

Figure 6. Hodograph for Larkhill (03743) at 0700 UTC on 11 January 1991. Winds shown are relative to the storm motion.

comma head at 0300 UTC. In general these show the cirrus outflow being carried to the north-east. However, Aberporth (which was near the centre of the comma head at 0700 UTC) has a relative wind of 135° 24 kn. This agrees well with the anticyclonically curved striations in the cirrus outflow. Although layered cloud is also present due to mass ascent within it, the comma head as seen by the satellite is mostly cirrus outflow from cumulonimbus clouds feeding into its southern flank. This is confirmed by the precipitation shown in the radar pictures.

Another notable feature was that individual storms in the Channel could be tracked for over 5 hours. To achieve this life-span, new cells were building into each storm, and this requires directional shear in the winds (see Bennetts *et al.**). Fig. 6 shows the Larkhill winds relative to a storm moving from 245° at 40 kn. With sea temperatures of 10 or 11 °C, convection would be from the surface. The low-level inflow is from the south-east quadrant, the cells lean to the north, and outflow is to the north-east. This can be inferred in some of the individual storms near the Larkhill plot in Fig. 2.

Using isentropic analysis and relative winds, a tentative conceptual model of the comma cloud is given in Fig. 2 (inset) showing the ascending conveyor belt.

J.R. Grant

* Bennetts, D.A., McCallum, E. and Grant, J.R.; Cumulonimbus clouds: an introductory review. *Meteorol Mag*, **115**, 1986, 242–256.

GUIDE TO AUTHORS

Content

Articles on all aspects of meteorology are welcomed, particularly those which describe results of research in applied meteorology or the development of practical forecasting techniques.

Preparation and submission of articles

Articles, which must be in English, should be typed, double-spaced with wide margins, on one side only of A4-size paper. Tables, references and figure captions should be typed separately. Spelling should conform to the preferred spelling in the *Concise Oxford Dictionary* (latest edition). Articles prepared on floppy disk (Compucorp or IBM-compatible) can be labour-saving, but only a print-out should be submitted in the first instance.

References should be made using the Harvard system (author/date) and full details should be given at the end of the text. If a document is unpublished, details must be given of the library where it may be seen. Documents which are not available to enquirers must not be referred to, except by 'personal communication'.

Tables should be numbered consecutively using roman numerals and provided with headings.

Mathematical notation should be written with extreme care. Particular care should be taken to differentiate between Greek letters and Roman letters for which they could be mistaken. Double subscripts and superscripts should be avoided, as they are difficult to typeset and read. Notation should be kept as simple as possible. Guidance is given in BS 1991: Part 1: 1976, and *Quantities, Units and Symbols* published by the Royal Society. SI units, or units approved by the World Meteorological Organization, should be used.

Articles for publication and all other communications for the Editor should be addressed to: The Chief Executive, Meteorological Office, London Road, Bracknell, Berkshire RG12 2SZ and marked 'For Meteorological Magazine'.

Illustrations

Diagrams must be drawn clearly, preferably in ink, and should not contain any unnecessary or irrelevant details. Explanatory text should not appear on the diagram itself but in the caption. Captions should be typed on a separate sheet of paper and should, as far as possible, explain the meanings of the diagrams without the reader having to refer to the text. The sequential numbering should correspond with the sequential referrals in the text.

Sharp monochrome photographs on glossy paper are preferred; colour prints are acceptable but the use of colour is at the Editor's discretion.

Copyright

Authors should identify the holder of the copyright for their work when they first submit contributions.

Free copies

Three free copies of the magazine (one for a book review) are provided for authors of articles published in it. Separate offprints for each article are not provided.

Contributions: It is requested that all communications to the Editor and books for review be addressed to the Chief Executive, Meteorological Office, London Road, Bracknell, Berkshire RG12 2SZ, and marked 'For *Meteorological Magazine*'. Contributors are asked to comply with the guidelines given in the *Guide to authors* which appears on the inside back cover. The responsibility for facts and opinions expressed in the signed articles and letters published in *Meteorological Magazine* rests with their respective authors.

Subscriptions: Annual subscription £33.00 including postage; individual copies £3.00 including postage. Applications for postal subscriptions should be made to HMSO, PO Box 276, London SW8 5DT; subscription enquiries 071–873 8499.

Back numbers: Full-size reprints of Vols 1–75 (1866–1940) are available from Johnson Reprint Co. Ltd, 24–28 Oval Road, London NW1 7DX. Complete volumes of *Meteorological Magazine* commencing with volume 54 are available on microfilm from University Microfilms International, 18 Bedford Row, London WC1R 4EJ. Information on microfiche issues is available from Kraus Microfiche, Rte 100, Milwood, NY 10546, USA.

March 1991

Editor: F.E. Underdown
Editorial Board: R.J. Allam, R. Kershaw, W.H. Moores, P.R.S. Salter

Vol. 120
No. 1424

Contents

ISSN 0026–1149

Printed in the United Kingdom for HMSO
Dd 0291241 C13 03/91 0503 12521